Urban Sensing of Virtual Internet of Things for Metaverse

Jiaxi Wang, Yixue Hao, *Member, IEEE*, Long Hu, Giancarlo Fortino, *Fellow, IEEE*, Salman A. Alqahtani, and Min Chen, *Fellow, IEEE*

***Abstract*—Urban sensing encourages the incredibly quick advancement of digitalization, intelligence, and ubiquitous perception, accelerating the construction of the metaverse. Various sensors construct the sensing network to capture human activities for the human-centered metaverse. However, effective management of ubiquitous urban sensing with various attributes is a challenge. In this article, we propose a virtual Internet of Things (VIoT) enabled by digital twin (DT) for building the metaverse. Specifically, we introduce an architecture of the VIoT, including a policy sensing layer, a 6G edge-cloud collaboration layer, a DT layer, and a user-friendly terminal layer. Furthermore, to address the sensing scheduling issue in the VIoT, we formulate a sensing profit maximization problem by considering the sensing coverage, data utility, and energy cost attributes of visual sensors and fabric sensors. To tackle this problem efficiently, we design a sensing scheduling policy based on the soft actor–critic (SSP-SAC) algorithm. The simulation results demonstrate that compared to the baseline schemes, the SSP-SAC scheme can significantly improve the sensing profit in diverse situations, indicating that the VIoT can provide an effective urban sensing policy.**

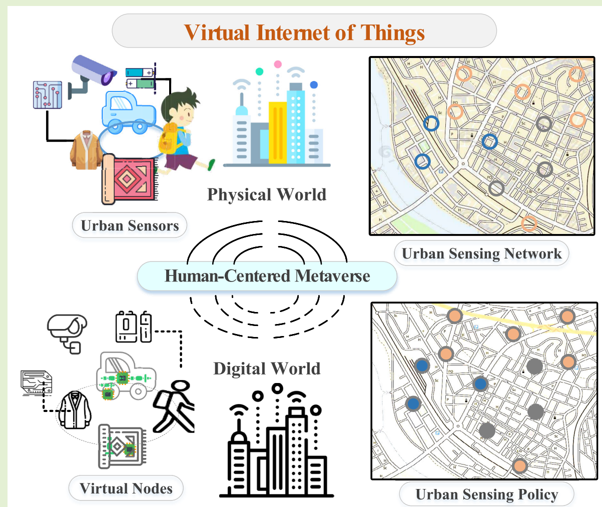

***Index Terms*— Digital twin (DT), metaverse, soft actor–critic, urban sensing.**

I. Introduction

URBAN sensing, powered by a variety of sensors and ubiquitous intelligence interconnects, is a collection of technologies for multidimensional and multilevel monitoring of the physical environment and social activities [1]. Urban sensors collect static and dynamic attributes used for urban analysis [2], for example, land cover and use, buildings, crowds [3], air qualities [4], or individuals of the city. Metaverse is a virtual digital world that includes simulated real-world environments and artificially created virtual spaces [5]. In the metaverse, participants engage in diverse activities and interact with others just like in the real world. Thus, the metaverse requires sensing the large-scale urban environment for the fidelity virtual simulation of the virtual worlds and real-time human activities sensing for immersive interaction [6].

Fortunately, urban sensing is a key enabler for the construction of metaverse, which supports the real-time and dynamic perception of urban activities [5]. The development of urban sensing technology promotes the extremely rapid development of digitalization, intelligence, and ubiquitous perception, which also accelerates the data-driven metaverse of the smart city [7]. With distinctive features of the immersive experience and sociality, modeling human-centered spaces is vital in the metaverse, including human activities and the human-around environment [8].

Manuscript received 4 September 2023; revised 3 December 2023; accepted 10 December 2023. Date of publication 3 January 2024; date of current version 29 February 2024. This work was supported by Distinguished Scientist Fellowship Program (DSFP2024), King Saud University, Riyadh, Saudi Arabia. The associate editor coordinating the review of this article and approving it for publication was Dr. Gautam Srivastava. *(Corresponding authors: Yixue Hao; Long Hu; Min Chen.)*

Jiaxi Wang, Yixue Hao, and Long Hu are with the School of Computer Science and Technology, Huazhong University of Science and Technology, Wuhan 430074, China (e-mail: jiaxiwang@hust.edu.cn; yixuehao@hust.edu.cn; hulong@hust.edu.cn).

Giancarlo Fortino is with the Department of DIMES, University of Calabria, 87036 Rende, Italy (e-mail: giancarlo.fortino@unical.it).

Salman A. Alqahtani is with the Department of Computer Engineering, College of Computer and Information Sciences, King Saud University, Riyadh 11574, Saudi Arabia (e-mail: salmanq@ksu.edu.sa).

Min Chen is with the School of Computer Science and Engineering, South China University of Technology, Guangzhou 510006, China, and also with the Pazhou Laboratory, Guangzhou 510330, China (e-mail: minchen@ieee.org).

Digital Object Identifier 10.1109/JSEN.2023.3347423

Human-centered urban sensing can be achieved by ambient intelligence and fabric computing [9]. First, as a part of urban sensing, ambient intelligence is a physical space that is sensitive and responsive to the presence of humans, which is driven by advances in machine learning and contactless sensors [10], such as visual sensors to perceive the human-centered environment and activities. However, the mild movement and lively signals are difficult to recognize, for example, occluded movements and pulse. On the contrary, fabric computing [11], based on micro and flexible sensors, creates a new paradigm of human-centered perception. It enables seamless human activity modeling in living spaces by deploying ubiquitous and ultradense fiber sensors to capture human physiological information [12], behavioral states, and interaction commands [13]. Nevertheless, it is difficult to accomplish wide capture like the visual sensors. Thus, various types of urban sensors are used for sensing the environment and human activities to construct the urban metaverse. For example, the visual sensors are responsible for monitoring the crowd flow situation and human surrounding changes [14], while the fabric and wearable sensors monitor the human-closed physiological signals and precise movements. Besides, other types of sensors such as gas sensors [15] and voice sensors [16] are utilized to realize the entire city modeling.

Therefore, the increasing of various types of urban sensors deployed in the city raises concerns about the reasonable sensing policy of large-scale deployment. Moreover, for fabric sensors, using machine learning and deep learning for pattern monitoring and recognition requires powerful computing capability [17]. Due to their convenient, micro, and flexible attributes, wearable devices are limited in terms of computing resources. The Internet of Things (IoT) promotes the development of human–computer interaction and smart cities [18]. However, the explosive growth of urban sensor types and densities poses a challenge for the classical IoT architecture to achieve large-scale sensing scheduling and management. Efficiency, self-adaption, and error tolerance are the urgent requirements for the advanced IoT [19]. Furthermore, the metaverse envisions the utilization of physical IoT devices to enable human interaction within the metaverse, thereby demanding the comprehensive digitization of the physical world [20]. Thus, the urban sensing network requires digital technology to fully digitize the physical urban sensing network, promoting large-scale sensing scheduling, and building a bridge between the physical world and the digital world.

Digital twin (DT) promotes the development of digital interaction and management [21], which integrates models, data, and intelligence for real-time, efficient, and intelligently controlled services [22]. If provided sufficient sensing coverage, data availability, and computational processing capacity, DTs can model sensing networks and make predictions about their behavior over time and under different conditions and constraints [23]. DT offers an entire life cycle evolution of the sensing network, which is advantageous for developers of deployment plan optimization, remote monitoring, and maintenance [24]. It facilitates predictive maintenance, service improvements, and fault diagnosis for operators [25]. Meanwhile, it offers intelligent, tailored, and immersive service experiences to users. Powered by various types of urban sensors and DT, the urban metaverse can create a new generation of hyperreality services and transform all ways of life [26]. Considering the different attributes of various types of sensors such as energy-saving or high-consumption, an effective cooperation sensing strategy assisted by DT is required for efficient urban sensing. It is urgent to develop an architecture and a sensing scheduling scheme to realize precise human-centered modeling and effective urban sensing management.

In this article, we propose a virtual IoT (VIoT) enabled by DT to construct the urban metaverse, in which the sensing nodes are mapped in the digital world. Specifically, we introduce the architecture of VIoT, including a policy sensing layer, a 6G edge-cloud collaboration layer, a DT layer, and a user-friendly terminal layer. Furthermore, to address the issue of sensing scheduling with various types of urban sensors, we formulate a sensing profit maximization problem by considering the sensors' attributes, which consist of sensing coverage, data utility, and energy cost. Moreover, to tackle this problem, we propose a sensing scheduling policy based on the soft actor–critic (SSP-SAC) algorithm deployed in VIoT for effective sensing management. Finally, we construct extensive experiments to evaluate the performance of the proposed scheme.

In summary, the contributions of this article include the following.

1) We propose a VIoT enabled by DT and urban sensors for constructing the urban metaverse. Moreover, we introduce an architecture of the VIoT, including a policy sensing layer, a 6G edge-cloud collaboration layer, a DT layer, and a user-centric terminal layer.
2) Considering the various attributes of urban sensors in the VIoT, we formulate a sensing profit maximization problem to address the effective sensing scheduling issue. To tackle this problem, we design a novel SSP-SAC algorithm deployed in the VIoT, which can adapt to dynamic environments.
3) To evaluate the performance of SSP-SAC over diverse situations, we conduct extensive experiments considering the sensing coverage, data utility, and energy cost of visual sensors and fabric sensors. The experimental results demonstrate that the SSP-SAC can significantly improve the sensing profit compared to the other schemes.

The rest of this article is organized in the following. Section II introduces the VIoT and its architecture. Section III formulates a sensing scheduling problem on maximizing sensing profit considering the various attributes of sensors. Section IV describes the proposed SSP-SAC algorithm. The comparison experiments are presented in Section V. Section VI concludes the whole article.

Types	Energy Cost	Sensing Coverage	Data Utility	Invisible Sensing
Visual Sensors	High	**High**	**High**	**High**
	Large amounts of data cost high collection and transmission energy.	Usually coveraging wide vision.	Collecting abundant information and multi-role sensing data.	Remote and uncontact sensing.
Fabric Sensors	**Low**	Low	Low	**High**
	Lightweight data costs less on collection and transmission.	Usually collecting the signal of a person.	Usually designed for specific tasks.	Being close to users and easy to sense subtle signals.

Fig. 1. Attributes of visual sensors and fabric sensors.

II. Architecture of VIoT

In this section, we analyze the attributes of urban sensors. Then, we introduce the VIoT based on DT and the architecture of VIoT, including a policy sensing layer, a 6G edge-cloud collaboration layer, a DT layer, and a user-friendly terminal layer.

A. Urban Sensors

Various types of urban sensors are deployed in the city. The fabric sensors are realized by conductive active materials that can be stretched, pulled, bent, and folded [27]. On the one hand, fabric sensors convert various physiological signals into electrical signals through flexible sensors, such as blood pressure, respiration [28], pulse, and heartbeat. The fabric sensors can be used for continuous, noninvasive, real-time, and comfortable monitoring that provides important clinically relevant information for disease diagnosis, preventive care, and rehabilitation care. On the other hand, fabric sensors convert human behavior information into digital signals, such as gestures, and human motion, which provides imperative support for multimodal senseless interactions [29]. Otherwise, as fundamental physical signal collectors, fabric sensors can be used to reprogram for additional goals and scopes based on the same types of fibers. For example, the intelligent gloves can be used to replicate the gesture in the metaverse or correct the gesture in the gesture-based education [30], [31]. Visual sensors [32] are the fundamental sensors in the city, which can capture abundant information about the environment and people. It can be used to assist in traffic management, pedestrian safety, public security, and urban environment monitoring. We compare the attributes of the visual and fabric sensors, as shown in Fig. 1.

1) *Energy Cost:* The visual sensors collect images and videos, which cost massive transmission energy and computing energy. Meanwhile, lightweight data generated by the fabric sensor costs less on computing, storage, and communication energy [33]. Therefore, the fabric sensors are low-cost [34] but the visual sensors are high-cost relatively.
2) *Invisible Sensing:* The fabric sensors can inadvertently and ubiquitously gather data on human behavior and physiological data [27], including temperature, blood pressure, pulse, and other measurements. The visual sensors can capture the environment in a noncontact way. They both perform well in invisible sensing, but the visual sensors are good at wide sensing and the fabric sensors are excellent at capturing subtle body movements and physiological signals in individuals.
3) *Sensing Coverage:* Sensing coverage represents the scope or capability of sensor nodes within the monitoring area in the sensing network. It measures the ability of sensor nodes to effectively monitor and perceive the target area. The arrangement and density of sensor nodes directly affect the network's perceptual coverage range. The visual sensors usually have a wide vision but the fabric sensors usually serve a certain user. Thus, the visual sensors perform in wide sensing coverage but the fabric only covers a person [35], [36], [37].
4) *Data Utility:* The visual sensors can capture more abundant information including human movement and the environmental changes. Moreover, the sensing data collected by visual sensors can be used for multiple tasks. For example, an image can be used for object recognition, pose recognition, and facial recognition. However, the fabric sensors are usually designed for specific tasks [38], for example, respiration monitoring and human movement monitoring.

In conclusion, due to different types of sensors having various attributes, reasonable and effective management can significantly maximize their value and improve the performance of the sensing network.

B. Definition of VIoT

VIoT is a digital mapping of the urban sensing network enabled by DT, as shown in Fig. 2. The physical city with various sensor nodes monitors the urban environment and human activities. Thus, if the sensor nodes are digitalized by modeling, visualization, and machine learning, not only are the sensing status synchronized in DT, but also the sensing data can be utilized to simulate the real city. As a result, the physical sensing nodes have virtual nodes in the virtual city, which is the virtual connotation of the VIoT. Physical sensing nodes are mapped one-to-one in a virtual city, and then spatial states, human behavior, and information communication are

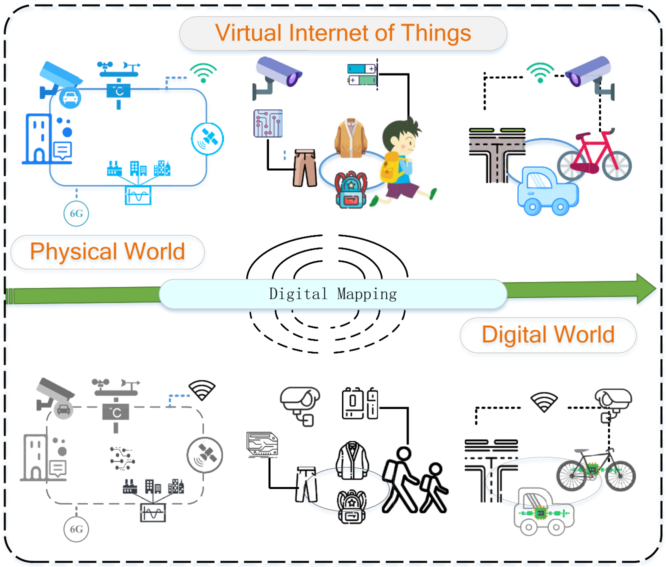

Fig. 2. Virtual IoT.

transformed into multidimensional models in the digital city. The physical city and the digital city will combine and exchange multimodal data.

The difference between VIoT and IoT [39] is that the VIoT has the mapping of the IoT enabled by DT. The DT can monitor, control, and improve physical IoT operations, including developing models for assessing energy consumption, rationalizing resource allocation [40], and enhancing sensing scheduling. When used in particular contexts, VIoT performs intelligent analysis, future behavior prediction, and decision-making optimization, while also enabling the extension and enhancement of the real environment following effective simulation, description, and construction of the desired scenario, combining the composability and programmability of its construction process to iteratively optimize problem solutions and better solve real-world. The vast amount of historical data, the findings of the analysis, and user feedback can aid in the twin's development [41].

C. Architecture of VIoT

The architecture of VIoT is illustrated in Fig. 3, which includes a policy sensing layer for multiattribute sensors, a 6G edge-cloud collaboration layer for artificial intelligence (AI) services, a DT layer for surrealistic space, and a user-friendly terminal layer for immersive interaction.

1) Policy Sensing Layer: The policy sensing layer consists of all the sensing units and the auxiliary equipment to support data acquisition. Various types of urban sensors are deployed in the city to collect and monitor data related to urban operations and human activities, including weather sensors, air quality sensors, visual sensors, and fabric sensors. All types of sensors in the urban area are connected together and managed by the DT layer. Meanwhile, the sensing network follows the sensing schedule policy provided by the DT layer to realize effective data collection.

Fabric sensors collect multidimensional information [9] about the environment on a fine-grained scale using functional fibers that respond to sound, light, and electricity at the mechanistic level. To enable wide-area low-energy sensing and high-quality human behavior data gathering, fabric sensors are made by combining flexible sensors with fibers, which can record changes in physical quantities, such as pressure [42], elasticity, and electromagnetic interaction forces. Otherwise, the visual sensors collect visual information about the environment around them. According to the signal feature, the sensing distribution follows certain rules, such as the distribution of the focal region, the dot matrix, the warp, and weft cross. Finally, a large-scale, high-density sensing network is constructed using multiple types of sensors to capture multimodal fine-grained sensing properties to create a geographically scoped sensing field. A huge number of sensing nodes that produce a variety of physical signals make up the resulting sensing network. A compact, highly precise, and compatible peripheral sampling network is needed to accurately gather and interpret sensing data. The microcontroller unit is used as the control core to deploy the data decoding module and data cleaning module to filter noise and redundant data to reduce the cost of subsequent transmission.

2) 6G Edge-Cloud Collaboration Layer: The urban metaverse is enabled by ubiquitous sensing and intelligence, the edge and cloud are the primary fundamental construction of the city. The high-performance 6G edge-cloud collaboration layer with intelligent services is beneficial to realize the vision of a seamless, shardless, and interoperable metaverse [43]. The fundamental services include machine learning and AI technologies for adaptive data collection, model construction, and AI perception. First, to improve the high-value time series segments of the gathered data and finish higher order services like noise reduction and semantic extraction, a lightweight deep perception algorithm model is implemented, enabling high-performance and intelligent perception. Second, owing to low-latency transmission and powerful computing capabilities, the intelligent services for VIoT are deployed and executed in the edge or cloud servers. Moreover, as the inherent sociality of the metaverse, the information is exchanged in a wide area, requiring low-latency cloud computing.

3) DT Layer: The management of a large-scale sensing network in the urban area is a challenge. DT can monitor, manage, and optimize the physical sensing operations, aiming to achieve optimal management of the urban sensing network by modeling high-fidelity urban environment and optimizing decisions utilizing intelligent algorithms such as deep learning and reinforcement learning. The holistic network virtualization incorporates service-centric and user-centered networking from service provision and service demand, respectively. The pervasive network intelligence integrates AI into future networks from the perspectives of networking for AI and AI for networking, respectively [44]. The DT layer is also deployed in the edge server or cloud. The operating condition, ambient information, and all available sensing data in the VIoT physical world are mapped to digital counterparts. The logical objects accurately represent all the significant traits and qualities of the original objects in a specific application context. In the digital world, the VIoT nodes communicate and cooperate with others to complete challenging tasks. Assisted

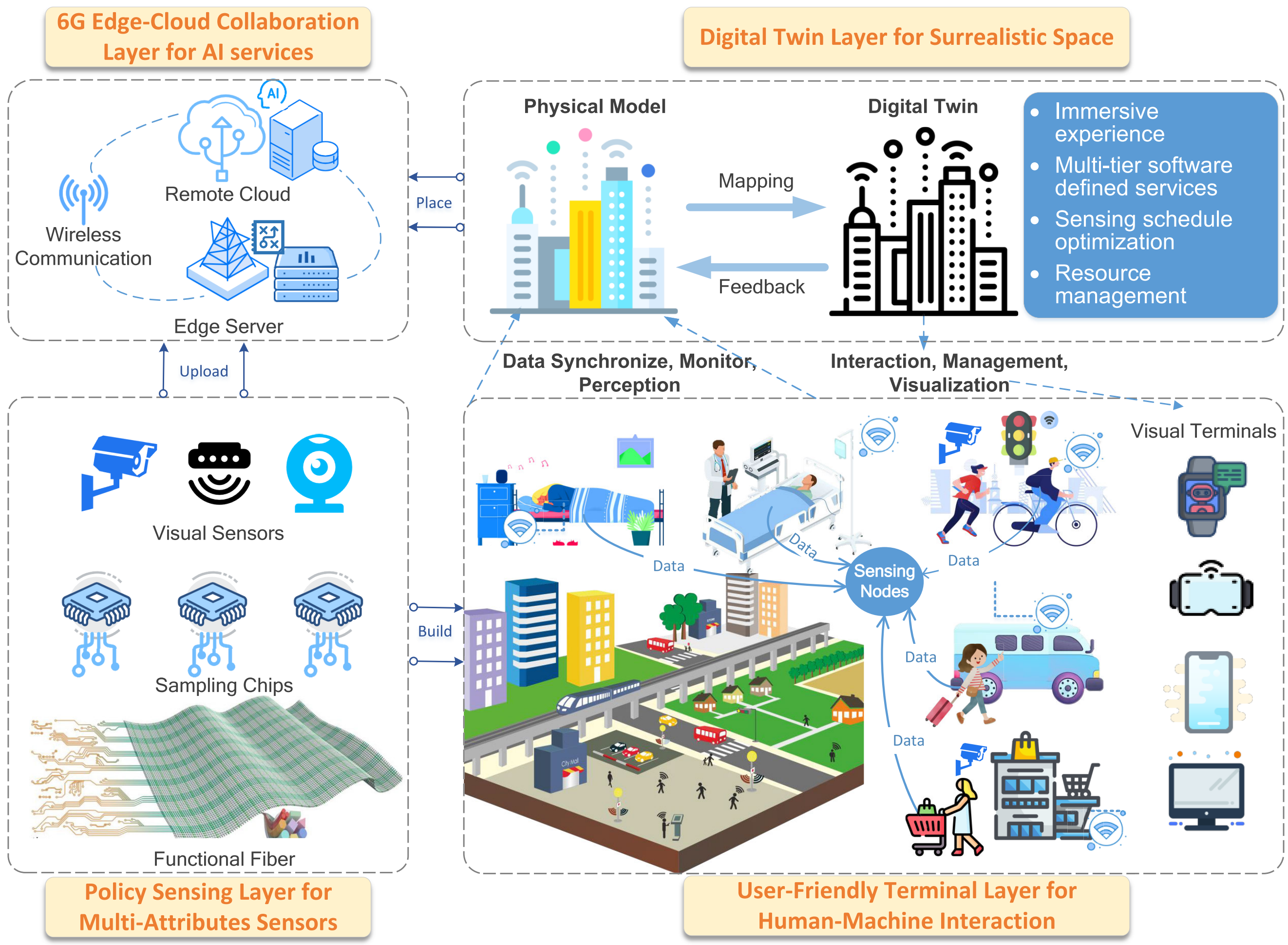

Fig. 3. Architecture of VIoT.

by DT, the VIoT can provide an immersive experience, multi-tier software-defined services, sensing schedule optimization, and resource management [45].

4) User-Friendly Terminal Layer: A service terminal ultimately offers service interfaces and direct interaction ways for users, including intelligent fabric devices like smart beds and clothes, and electronic devices like smartphones, virtual reality glasses, and personal computers. The two types of intelligent terminals cooperate to provide users with an engaging experience. The fabric devices are close to users with interaction and feedback, while the electronic devices display the visualization of virtual scenes. Being a connection of reality to the virtual world, both the digital scene reproduction and immersive interaction are provided in the user-friendly terminal layer.

In summary, VIoT employs ubiquitous sensing nodes to gather a variety of behavioral and spatial data in a particular scene, which is then individually mapped in the digital space. Based on the virtual-realistic symbiotic network with ubiquitous senseless interaction, it creates an immersive interaction space for users to improve their experience and comfort.

III. System Model and Problem Formulation

In this section, we formulate a DT-assisted sensing scheduling problem to optimize sensing profit considering sensing coverage, data utility, and energy cost of visual sensors and fabric sensors.

A. System Overview

The system model contains a physical sensing layer and a DT layer, as shown in Fig. 4. In the physical layer, the sensing nodes collect and transmit data to the nearest edge cloud by wireless or wired ways. On the edge cloud, the DT makes the optimal decision by observing the status of the physical sensing network and managing the sensing schedule. The physical sensing network and DT exchange the data and decisions timely.

The various types of urban sensors are deployed in the city. The sensing region is discretized into N cells, denoted as $\mathcal{N} = \{1, 2, \ldots, N\}$. The cells can be arbitrary shapes, but we assume that they have the same size for simplicity. To prioritize human-centered urban sensing, we divide the sensors into visual sensors and fabric sensors to collect data on human surroundings and activities. We denote the set of M visual sensors as X^v. Wearable devices are usually constructed by some sensors, thereby we define x_k^f as a representation of all of the fabric sensors on a wearable device. Thus, X^f represents the K wearable devices. The sets of the sensors can

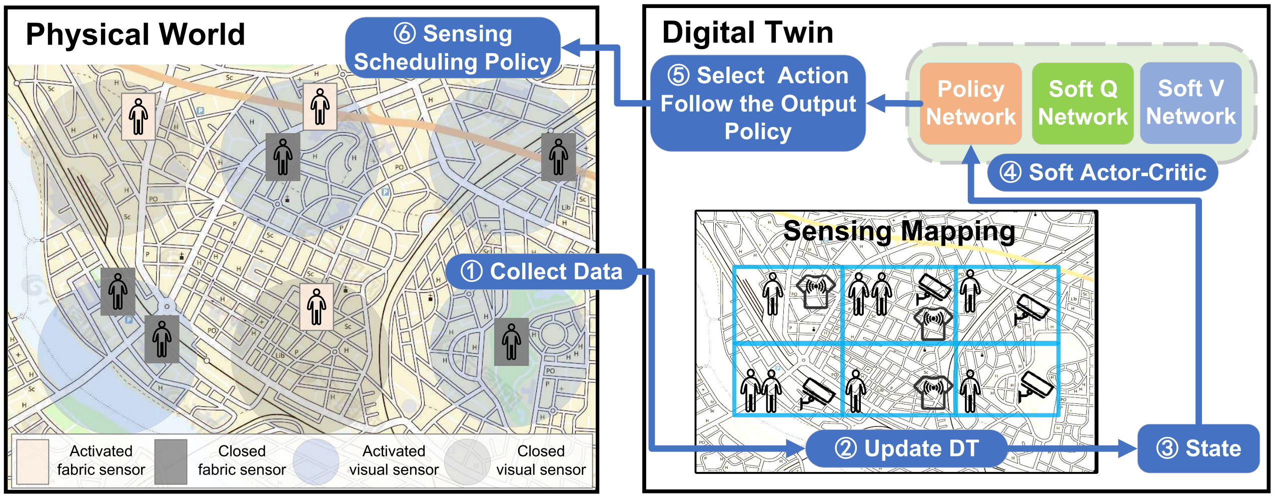

Fig. 4. System framework for sensing scheduling policy.

be denoted as

$$\begin{cases} X^v = \left\{x_1^v, x_2^v, \ldots, x_M^v\right\} \\ X^f = \left\{x_1^f, x_2^f, \ldots, x_K^f\right\}. \end{cases} \tag{1}$$

The visual sensors are usually fixed but the wearable devices can be moved or fixed. Due to the visual sensors usually covering an area, we suppose a cell n has a visual sensor x_m^v, thereby we can get $N = M$. We define X^v and X^f as the sensors' on–off status, that if $x_m^v = 1$ or $x_k^f = 1$ means the mth and kth sensors are activated and collecting data, else are closed.

The sensing profit of the sensing scheduling can be defined by sensing benefit and cost. Each type of sensor has unique attributes, resulting in different benefits and costs. We evaluate the sensing benefit from two perspectives: sensing coverage and data utility [46]. The sensing coverage indicates the capability of a sensor for data collection, and the data utility indicates how useful or redundant the collected data is. We define q_v and q_f as the data utility indicators for the visual sensors and fabric sensors. Otherwise, we evaluate the sensing cost through the energy consumption caused by the sensors and the sensing data, which contains the sensors working consumption and data transmission consumption. We define the e_v and e_f as energy cost indicators for visual sensors and fabric sensors.

B. DT Model

The DT layer is deployed on the edge cloud which replicates the sensing nodes and the edge cloud, and updates the time-variant state information, historical data, and scheduling strategy. By synchronizing the overall situation, such as the users' position and the sensors' state, the DT makes the optimal sensing scheduling strategies for the physical sensing layer. The DT layer consists of the city cells DT^N and the status of visual sensors DT^v and fabric sensors DT^f, which can be expressed as

$$\mathrm{DT} = \left(\mathrm{DT}^N, \mathrm{DT}^v, \mathrm{DT}^f\right). \tag{2}$$

The DT duplicate of city cells DT^N is denoted as

$$\mathrm{DT}^N = \{u_1, u_2, \ldots, u_N\} \tag{3}$$

where u_n is the number of the users in the nth cell of city. The mth visual sensor duplicate DT_m^v can be expressed as

$$\mathrm{DT}_m^v = \Phi\left(c_v, q_v, e_v, x_m^v\right) \tag{4}$$

where c_v, q_v, and e_v are the sensing coverage, data utility, and energy cost, respectively. Similarly, the kth wearable device duplicate DT_k^f can be expressed as

$$\mathrm{DT}_k^f = \Phi\left(c_f, q_f, e_f, x_k^f\right) \tag{5}$$

where c_f, q_f, and e_f are the sensing coverage, data utility, and energy cost, respectively. For a human-centered urban sensing network, we define the sensing coverage as the number of covered users by a sensor. Due to the number of cells N is the same as the number of visual sensors M, namely $M = N$, the number of users u_n in the nth cells can also be expressed as u_m in the mth cell. Therefore, the total sensing coverage $\mathcal{G}_c$, data utility $\mathcal{G}_q$, and energy cost $\mathcal{G}_e$ can be expressed as

$$\begin{cases} \mathcal{G}_c = \sum_{m=1}^{M} x_m^v u_m + \sum_{k=1}^{K} x_k^f \\ \mathcal{G}_q = \sum_{m=1}^{M} q_v x_m^v u_m + \sum_{k=1}^{K} q_f x_k^f \\ \mathcal{G}_e = \sum_{m=1}^{M} e_v x_m^v + \sum_{k=1}^{K} e_f x_k^f \end{cases} \tag{6}$$

where $x_m^v u_m$ means the visual sensor can cover and collect all of the users in the mth cell.

C. Problem Formulation

With the aforementioned assumptions and terms, we formulate the sensing scheduling problem as follows.

In the city which is divided into N cells, given the number of users of each cell DT^N, determine the on–off status of visual sensors X^v and fabric sensors X^f that optimizes the sensing profit $\mathcal{G}$, which is defined as the benefit minus cost, subject to the sensors configuration and users activate space constraints. Formally, this is stated as

$$\mathcal{P}_1 : \mathcal{G} = \max_{X^v, X^f} \mathcal{G}_c + \mathcal{G}_q - \mathcal{G}_e \tag{7}$$

$$\text{s.t. } C1 : x_m^v, x_k^f \in \{0, 1\} \tag{8}$$

$$C2 : \sum_{n=0}^{N} u_n = K. \tag{9}$$

The optimization goal is to maximize the sensing profit by a sensing scheduling scheme. Constraint $C1$ means that the sensors activated status. Constraint $C2$ means that the number of users is equal to the number of wearable devices. This formulation of the sensing scheduling problem is a typical integer programming problem known as NP-hard.

IV. Sensing Scheduling Policy Based on Soft Actor–Critic Network

In this section, we propose an SSP-SAC algorithm. Specifically, we formalize the optimization problem as a Markov decision process (MDP) and display the algorithm analysis and details.

A. Formalization of MDP

It is generally believed that the variation of the sensing environments follows Markovian properties. The three key elements of the learning environment system, i.e., the set of states S, the set of actions A, and the set of reward functions R.

State: At each time slot t, the state of the urban sensing network can be represented as

$$s_t = \left\{ \mathrm{DT}_t^N, \sum_{m=1}^{M} x_{m,t}^v, \sum_{k=1}^{K} x_{k,t}^f, \mathcal{G}_{c,t}, \mathcal{G}_{q,t}, \mathcal{G}_{e,t} \right\} \tag{10}$$

where $\sum_{m=1}^{M} x_{m,t}^v$ and $\sum_{k=1}^{K} x_{k,t}^f$ mean the number of activated sensors at time slot t. $\mathcal{G}_{c,t}$, $\mathcal{G}_{q,t}$, and $\mathcal{G}_{e,t}$ denote the total sensing coverage, data utility, and energy cost at time slot t.

Action: Based on the current state s_t, the agent chooses the action a_t, which can be expressed as

$$a_t = \left\{ X_t^v, X_t^f \right\} \tag{11}$$

where X_t^v in $[1, M]$ dimension and X_t^f in $[1, K]$ dimension denote the sensors activated state at time slot t.

Reward: The reward function R presents the system sensing profit obtained by the sensing scheduling policy. According to the current system state s_t and the chosen action a_t at time slot t, the reward can be expressed as

$$r_t = \mathcal{G}_{c,t} + \mathcal{G}_{q,t} - \mathcal{G}_{e,t}. \tag{12}$$

The set of reward functions $R = \{r_t | t \in [1, T]\}$ is the system rewards in all time slots $t \in [1, T]$. Our goal is to maximize the cumulative reward.

B. Soft Actor–Critic for Sensing Scheduling Policy

Since the action space is composed of 0 or 1 in total $N + K$ dimensions, lots of final actions are possible to achieve optimal rewards. The agent is expected to explore sufficiently for the wider possibilities to avoid local optimum. SAC [47] attempts to find a policy that maximizes the maximum entropy objective. It has powerful exploration, robustness, and generalization abilities by exploring multimodal rewards and optimal possibilities in different ways. SAC can effectively solve the sensing scheduling problem because it can explore all possible actions by random policy.

The maximum entropy objective of SAC can be expressed as

$$\pi^* = \underset{\pi}{\operatorname{argmax}} \sum_{t=0}^{T} E_{(s_t, a_t) \sim \tau_\pi} \left[\gamma^t \left(r\left(s_t, a_t\right) + \alpha \mathcal{H}\left(\pi\left(. \mid s_t\right)\right) \right] \tag{13}$$

where π is a policy, π^* is the optimal policy, T is the number of timesteps, $r : S \times A \to R$ is the reward function, $\gamma \in [0, 1]$ is the discount rate, $s_t \in S$ is the state at timestep t, $a_t \in A$ is the action at timestep t, τ_π is the distribution of trajectories induced by policy π, α determines the relative importance of the entropy term versus the reward and is called the temperature parameter, and $\mathcal{H}(\pi(. \mid s_t)$ is the entropy of the policy π at state s_t and is calculated as $\mathcal{H}(\pi(. \mid s_t)) = -\log \pi(. \mid s_t)$.

Since the action in this article is discrete, we use the output policy by SAC as the probability of the discrete action

$$a_{t,i^*} \in \{0, 1\} \sim \pi_{i^*,t} \quad \forall i \in \{1, 2, \ldots, N + K\}. \tag{14}$$

The SAC algorithm consists of three types of networks, i.e., target value network, Q-function network, and policy network. First, to maximize the objective, SAC uses soft policy iteration which is a method of alternating between policy evaluation and policy improvement within the maximum entropy framework. The soft state value function can be expressed as

$$V\left(s_t\right) = E_{a_t \sim \pi} \left[Q\left(s_t, a_t\right) - \alpha \log\left(\pi\left(a_t \mid s_t\right)\right) \right]. \tag{15}$$

We can obtain the soft q-function by parameterizing the soft q-function $Q_\phi(s_t, a_t)$ using a neural network with parameters ϕ. Then, we train the soft Q-function to minimize the soft Bellman residual

$$J_Q(\phi) = r + \gamma \left(Q_\phi\left(s', a'\right) - \alpha \log \pi_\theta\left(a' | s'\right) \right), a' \sim \pi\left(\cdot | s'\right) \tag{16}$$

where a' and s' give the next state and action sample from the experience pool. Then, we can update the Q-network parameters by

$$\nabla_\phi E_B \sum_{i=1}^{B} \left(Q_\phi(s, a) - J_Q(\phi) \right)^2 \tag{17}$$

where E means the expectation of the sampled experience transition.

The policy network is used to predict the optimal policy and action π_t, a_t by the state s_t. It updates the policy for maximizing the rewards r. The SAC utilizes the soft Q-function calculated in the policy evaluation step to guide the policy changes. Specifically, it updates the policy toward the exponential of the new soft Q-function and restricts the

Algorithm 1 Soft Actor–Critic for Sensing Scheduling Policy

Require: The number of city cells N, visual sensors M and fabric sensors K, EPISODES, the batchsize B, $maxstep$

Initialize policy parameters θ, Q-function parameters ϕ_1, ϕ_2, set target parameters equal to main parameters $\phi_{tar,j} \leftarrow \phi_j$, $j = 1, 2$

for episode in range(EPISODES) **do**

  Random $DT^N = \{u_1, \ldots, u_N\}$ where $\sum DT^N = K$

  Random $X^v = \{x_1^v, \ldots, x_M^v, x_m^v \in \{0, 1\}\}$ and $X^f = \{x_1^f, \ldots, x_K^f, x_k^f \in \{0, 1\}\}$

  Get the state $s_t = \{DT_0^N, \sum X_0^f, \sum X_0^v, \mathcal{G}_{c,0}, \mathcal{G}_{q,0}, \mathcal{G}_{e,0}\}$

  for i in range($maxstep$) **do**

    Use policy network to output the probability of action by $\pi(a_t|s_t) = \Phi_\pi(\phi)(X_t)$

    Get the action by $a_t = 0$ if $a_t \leq 0.5$ else 0

    Get X_t^f and X_t^v according $a_t = \{X_t^f, X_t^v\}$

    Get the benefits $\mathcal{G}_{c,t}$, $\mathcal{G}_{q,t}$, cost $\mathcal{G}_{e,t}$ and reward r_t by s_t and a_t using Equation (6) and (14)

    Get the next state s_{t+1}

    Store transition tuple $(s_t, \pi_t, a_t, r_t, s_{t+1})$ in $\mathcal{B}$

    if $len(\mathcal{B}) \geq B$ **then**

      Sample B transition (s, π, a, r, s') from $\mathcal{B}$

      Compute targets for the Q function $a' \sim \pi(\cdot|s')$: $y_j = r_j + \gamma(\min_{j=1,2} Q_\phi(s', a') - \alpha \log \pi_\theta(a'|s'))$

      Update Q-functions for:

$$\nabla_\phi \frac{1}{B} \sum_{i=1}^{B} \left(Q_\phi(s, a) - y_j^2 \right), \; j = 1, 2$$

      Update policy network parameter:

$$\nabla_\phi \frac{1}{B} \sum_{i=1}^{B} \left(\min_{j=1,2} Q_\phi(s, \tilde{a}_\theta(s) - \alpha \log \pi_\theta(\tilde{a}_\theta(s)|s)) \right)$$

      where $\tilde{a}_\theta(s)$ is a sample from $\pi(\cdot|s')$.

      Update target networks with $\phi_{tar,j} \leftarrow \rho\phi_{tar,j} + (1 - \rho)\phi_{tar,j}$

    else

      Continue

    end if

  end for

end for

possible policies to a Gaussian distribution. The overall policy improvement step is given by

$$\nabla_\phi E_B \left(Q_\phi(s, \tilde{a}_\theta(s) - \gamma \log \pi_\theta(\tilde{a}_\theta(s)|s)) \right). \tag{18}$$

The pseudocode of the SSP-SAC algorithm for the DT-assisted sensing network is given in Algorithm 1. First, input the required settings and initialize the network parameters. Randomly generate the number of users in each cell DT^N and initial action with seed. Second, use the policy network to output the probability of the action and put the action, policy, state, next state, and reward into the experience pool. Third, randomly sample the experience transition and update the Q-value network according to (17), the value network according to (15), and the policy value network according to (18), respectively. After training, we can use the policy network to predict the optimal policy for the sensing scheduling.

V. Experimental Results

In this section, we conduct comparison experiments to verify the characteristics of the VIoT and evaluate the performance of the proposed SSP-SAC algorithm. First, we perform the convergence of SSP-SAC to find the optimistic network parameter. Then, we show the comparison experiments over the varying cells and users to evaluate the generalization of SSP-SAC algorithm. Finally, we analyze the sensing profit over the varying utility and energy cost indicators to evaluate if the SSP-SAC can adapt the various attribute sensors.

A. Experimental Setting

We consider a DT-assisted urban sensing network with two types of sensors, fabric sensors and visual sensors. The attributes of sensors are different. The visual sensors can not only capture the activity of humans but also observe the environment around the users, thus the collected data may be used for multiple tasks. Moreover, one visual sensor can monitor more than one person. On the contrary, a wearable device or fabric sensing device constructed by fabric sensors is usually designed for a user, hence it has lower data utility. In terms of cost, fabric sensors collect a small size of data compared to visual sensors, thus the transmission energy consumption is lower than the visual sensors. In summary, the visual sensors perform the higher sensing coverage and data utility, but the fabric sensors perform the lower energy cost. Therefore, we use the indicators to reflect the difference in attributions of different sensors. We assume that the data utility and energy cost indicators of visual sensors are in the range of $q_v, e_v \in [1, 3]$ and one of the fabric sensors is $q_f, e_f \in [0.4, 1.2]$, in which the utility indicator and cost of visual sensors are both always higher than the fabric sensors. We assume that the city is divided into N cells and K users are in the city, and N and K are in the range of $[100, 300]$, respectively.

B. Experimental Performance

To evaluate the performance of the algorithm, we use the system accumulated reward R and average profit $\mathcal{G}$ of 50 times as the metrics. Then, we compare the proposed scheme to the other three schemes.

1) *Random:* Randomly generate the activated status for the sensing network.
2) *Visual:* All of the visual sensors are activated but fabric sensors are closed.
3) *Fabric:* All of the fabric sensors are activated but visual sensors are closed.

1) SSP-SAC Algorithm Convergence Analysis: The number of hidden nodes is the primary coefficient of the SAC network. We test the convergence with various coefficient sets to find the optimistic configuration. Fig. 5 illustrates the convergence trend of the training process, in which the longitudinal axis

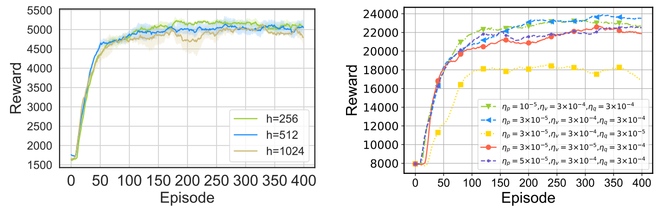

(a) (b)

Fig. 5. Convergence curve of the sensing scheduling policy algorithm. (a) Reward convergence curve over the varying hidden sizes. (b) Reward convergence curve over the varying learning rates.

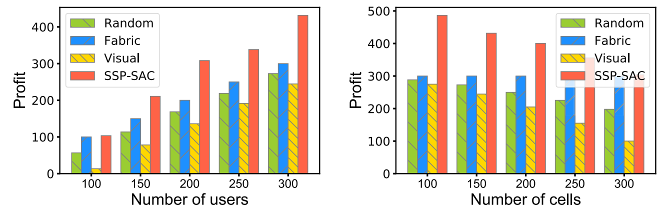

(a) (b)

Fig. 6. Impact on the number of cells and users. (a) Sensing profit over the varying numbers of users. (b) Sensing profit over the varying numbers of city cells.

indicates the accumulated reward R of a training round, which can be calculated by

$$R = \sum_{t=0}^{T} r_t. \tag{19}$$

Since the reward increases with fluctuation, we smooth the accumulated reward R which can be calculated by

$$R'_i = 0.9R'_{i-1} + 0.1R_i \tag{20}$$

where the R'_{i-1} means the weight accumulated reward of the last episode. For the fixed learning rate and $N = 100$, $K = 100$, it can be seen from Fig. 5(a) that the algorithm has converged after 100 epochs, and the higher hidden size results in a lower reward. But the converged speeds of all curves tend to be similar.

For the fixed hidden size $h = 512$, we adjust the learning rate of policy network η_p, value network η_v, and Q-function network η_q to find the optimistic parameters of the algorithm. We set the other parameters as $N = 100$, $K = 300$. It can be seen from Fig. 5(b) that the final convergence reward is lower than others obviously when $\eta_q = 3\times10^{-5}$, while others perform approximates closely. We can find that the configure $\eta_p = 3 \times 10^{-5}$, $\eta_v = 3 \times 10^{-4}$, and $\eta_q = 3 \times 10^{-4}$ is the best choice, which tends to 23 500 at epoch 400.

2) Impact on the Number of Cells and Users: Fig. 6 compares the profits $\mathcal{G}$ of SSP-SAC and the benchmark scheme over the varying number of users K and cells N. It can be seen that the SSP-SAC has more obvious optimization results. We set the same indicators that $q_v = 1$, $q_f = 0.5$, $e_v = 1.5$, and $e_f = 0.5$. For the fixed number of cells $N = 100$, as shown in Fig. 6(a), the profits of all of the schemes increase. This is because as the number of users increases, more fabric sensors and visual sensors create more sensing coverage. Meanwhile, the difference between fabric and visual becomes smaller, but the difference between the SSP-SAC and others becomes larger. The profits of SSP-SAC are always higher than others, the random is between the visual and fabric scheme, and the fabric is always higher than the visual scheme. When the number of users is the same as the number of cells $N = K = 100$, the profit of SSP-SAC is close to the fabric profit. Therefore, it can be concluded that with a higher number of users, the optimal performance becomes better. Otherwise, for the fixed number of users $K = 300$, it can be seen from Fig. 6(b) that the profits of the schemes decrease, as the number of cells increases, but the fabric profit is constant. Meanwhile, the difference between fabric and visual becomes larger, but the difference between the SSP-SAC and others becomes smaller. This is because the increase of cells does not change the number of fabric sensors, but increases the number of visual sensors. Thus, the benefit and cost of the fabric sensors remain constant. The profits of SSP-SAC are always higher than others, the random is between the visual and fabric schemes, and the fabric scheme is always higher than the visual scheme. When the number of users is the same as the number of cells $K = N = 300$, the profit of SSP-SAC is close to the fabric profit. Overall, we can conclude that the proposed SSP-SAC algorithm can improve the sensing profit when various types of sensors with different attributes are in the sensing network. The optimization performance becomes obvious when the difference between cells and users increases.

3) Impact on the Data Utility Indicators: Fig. 7 compares the profit $\mathcal{G}$ of the proposed algorithm and the benchmark scheme over the varying data utility indicators q_v and q_f. The varying data utility indicators mean the different data values of the collected sensing data, namely, the higher utility indicators mean the sensors can capture more useful and high-quality data. It can be seen that the profits increase as the indicators increase, which is because the higher data utility indicators lead to higher benefits. Moreover, the profits of SSP-SAC are higher than the other schemes in both Fig. 7(a) and (b); thus, it can be concluded that the proposed SSP-SAC can significantly improve the sensing profit over the varying attribution sensors. For the fixed data utility indicators of fabric sensors $q_f = 0.5$, as shown in Fig. 7(a), the fabric profit is constant and lower than the visual profit except for $q_v = 1.0$. For the fixed data utility indicators of visual sensors $q_v = 1.5$, as shown in Fig. 7(b), the fabric profit is constant and higher than the visual profit except for $q_f = 0.4$ and 0.6.

4) Impact on the Energy Cost Indicators: Fig. 8 compares the profits $\mathcal{G}$ of the proposed algorithm and the benchmark scheme over the varying energy cost indicators e_v and e_f. The varying energy cost indicators mean the different energy consumption performance of the sensors and the collected sensing data, namely, the higher energy indicators mean the sensors consume more energy consumption to complete the sensing tasks and the data transmission tasks. It can be seen that the profits decrease as the energy cost indicators increase, which is because the higher energy cost indicators lead to higher costs. Moreover, the profits of SSP-SAC are higher

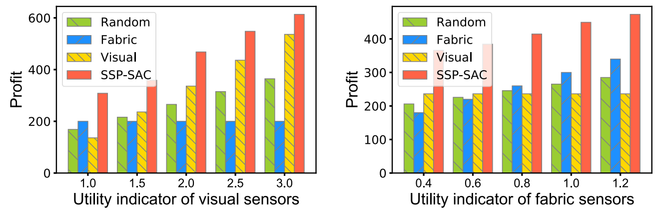

(a) (b)

Fig. 7. Impact on data utility indicators. (a) Sensing profit over the varying utility indicators of visual sensors. (b) Sensing profit over the varying utility indicators of fabric sensors.

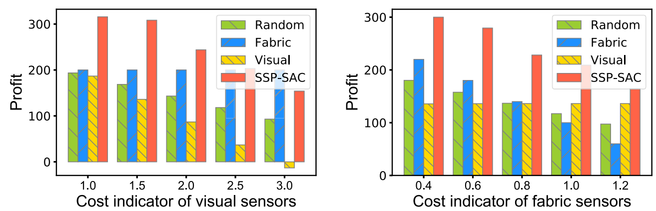

(a) (b)

Fig. 8. Impact of energy cost indicators. (a) Sensing profit over the varying energy cost indicators of visual sensors. (b) Sensing profit over the varying energy cost indicators of fabric sensors.

than other schemes in both Fig. 8(a) and (b); thus, it can be concluded that the proposed SSP-SAC can significantly improve the sensing profit over the varying attribution sensors. For the fixed energy indicators of fabric sensors $e_f = 0.5$, as shown in Fig. 8(a), the fabric profit is constant and higher than the visual profit. The visual profit when $e_v = 3.0$ is lower than 0 because of the high energy cost consumption. As we can see, the optimal performance is better when e_v is small, and it is best when $e_v = 1.0$. For the fixed energy cost indicator of visual sensors $e_v = 1.5$, as shown in Fig. 8(b), the visual profit is constant and lower than the fabric scheme except for $e_f = 1.0$ and 1.2.

VI. Conclusion

In this article, we proposed the VIoT based on the DT for building the urban metaverse. The multiple types of urban sensing nodes were mapped in the digital world in VIoT. Then, we introduced an architecture for building the VIoT, consisting of a policy sensing layer for multiattribute sensors, a 6G edge-cloud collaboration layer for AI services, a DT layer for surrealistic space, and a user-friendly terminal layer for human–machine interaction. Besides, we designed a sensing scheduling policy algorithm using the SAC called SSP-SAC, which considered the various attributes of sensors for human-centered sensing policy. Finally, we conducted extensive experiments to evaluate the proposed scheme. The experimental results demonstrate that the SSP-SAC can significantly improve the sensing profit compared to the other schemes. In summary, the various types of urban sensors in the VIoT are beneficial for capturing the multimode signals and creating a connection from the physical world to the urban metaverse. The VIoT can build the human-centered urban metaverse and the SSP-SAC can be used in the sensing policy optimization in the city to promote the development of urban sensing.

References

[1] T. Kliestik, M. Poliak, and G. H. Popescu, "Digital twin simulation and modeling tools, computer vision algorithms, and urban sensing technologies in immersive 3D environments," *Geopolitics, History, Int. Relations*, vol. 14, no. 1, pp. 9–25, 2022.

[2] H. Habibzadeh, Z. Qin, T. Soyata, and B. Kantarci, "Large-scale distributed dedicated- and non-dedicated smart city sensing systems," *IEEE Sensors J.*, vol. 17, no. 23, pp. 7649–7658, Dec. 2017.

[3] S. Ji, Y. Zheng, and T. Li, "Urban sensing based on human mobility," in *Proc. ACM Int. Joint Conf. Pervasive Ubiquitous Comput.*, Sep. 2016, pp. 1040–1051.

[4] J. Dutta, C. Chowdhury, S. Roy, A. I. Middya, and F. Gazi, "Towards smart city: Sensing air quality in city based on opportunistic crowd-sensing," in *Proc. 18th Int. Conf. Distrib. Comput. Netw.*, Jan. 2017, pp. 1–6.

[5] F. Tang, X. Chen, M. Zhao, and N. Kato, "The roadmap of communication and networking in 6G for the metaverse," *IEEE Wireless Commun.*, vol. 30, no. 4, pp. 72–81, Aug. 2023.

[6] K. Kuru, "MetaOmniCity: Toward immersive urban metaverse cyberspaces using smart city digital twins," *IEEE Access*, vol. 11, pp. 43844–43868, 2023.

[7] H. Xia, Z. Liu, M. Efremochkina, X. Liu, and C. Lin, "Study on city digital twin technologies for sustainable smart city design: A review and bibliometric analysis of geographic information system and building information modeling integration," *Sustain. Cities Soc.*, vol. 84, Sep. 2022, Art. no. 104009.

[8] A. T. Campbell, S. B. Eisenman, N. D. Lane, E. Miluzzo, and R. A. Peterson, "People-centric urban sensing," in *Proc. 2nd Annu. Int. Workshop Wireless Internet*, 2006, p. 18.

[9] C. Kaspar, B. J. Ravoo, W. G. van der Wiel, S. V. Wegner, and W. H. P. Pernice, "The rise of intelligent matter," *Nature*, vol. 594, no. 7863, pp. 345–355, Jun. 2021.

[10] A. Haque, A. Milstein, and L. Fei-Fei, "Illuminating the dark spaces of healthcare with ambient intelligence," *Nature*, vol. 585, no. 7824, pp. 193–202, Sep. 2020.

[11] M. Chen et al., "Fabric computing: Concepts, opportunities, and challenges," *Innovation*, vol. 3, no. 6, Nov. 2022, Art. no. 100340.

[12] A. Nag, S. C. Mukhopadhyay, and J. Kosel, "Wearable flexible sensors: A review," *IEEE Sensors J.*, vol. 17, no. 13, pp. 3949–3960, Jul. 2017.

[13] M. Chen et al., "Imperceptible, designable, and scalable braided electronic cord," *Nature Commun.*, vol. 13, no. 1, p. 7097, Nov. 2022.

[14] A. Pandharipande et al., "Sensing and machine learning for automotive perception: A review," *IEEE Sensors J.*, vol. 23, no. 11, pp. 11097–11115, Jun. 2023.

[15] D. Iskandaryan, F. Ramos, and S. Trilles, "Air quality prediction in smart cities using machine learning technologies based on sensor data: A review," *Appl. Sci.*, vol. 10, no. 7, p. 2401, Apr. 2020.

[16] Y. Su, K. Ma, X. Zhang, and M. Liu, "Neural network-enabled flexible pressure and temperature sensor with honeycomb-like architecture for voice recognition," *Sensors*, vol. 22, no. 3, p. 759, Jan. 2022.

[17] Y. Hao, L. Hu, and M. Chen, "Joint sensing adaptation and model placement in 6G fabric computing," *IEEE J. Sel. Areas Commun.*, vol. 41, no. 7, pp. 2013–2024, Jul. 2023.

[18] K. K. kumar, E. Ramaraj, and D. Indira, "Data fusion method and Internet of Things (IoT) for smart city application," in *Proc. 3rd Int. Conf. Intell. Commun. Technol. Virtual Mobile Netw. (ICICV)*, Feb. 2021, pp. 284–289.

[19] A. K. Sangaiah, A. Javadpour, F. Ja'fari, H. Zavieh, and S. M. Khaniabadi, "SALA-IoT: Self-reduced Internet of Things with learning automaton sleep scheduling algorithm," *IEEE Sensors J.*, vol. 23, no. 18, pp. 20737–20744, Sep. 2023.

[20] Y. Zhou, H. Huang, S. Yuan, H. Zou, L. Xie, and J. Yang, "MetaFi++: WiFi-enabled transformer-based human pose estimation for metaverse avatar simulation," *IEEE Internet Things J.*, vol. 10, no. 16, pp. 14128–14136, Aug. 2023.

[21] L. U. Khan, W. Saad, D. Niyato, Z. Han, and C. S. Hong, "Digital-twin-enabled 6G: Vision, architectural trends, and future directions," *IEEE Commun. Mag.*, vol. 60, no. 1, pp. 74–80, Jan. 2022.

[22] H. Chen, Z. Zhang, P. Karamanakos, and J. Rodriguez, "Digital twin techniques for power electronics-based energy conversion systems: A survey of concepts, application scenarios, future challenges, and trends," *IEEE Ind. Electron. Mag.*, vol. 17, no. 2, pp. 20–36, Nov. 2023.

[23] A. Tzachor, S. Sabri, C. E. Richards, A. Rajabifard, and M. Acuto, "Potential and limitations of digital twins to achieve the sustainable development goals," *Nature Sustainability*, vol. 5, no. 10, pp. 822–829, Jul. 2022.

[24] G. Caprari, G. Castelli, M. Montuori, M. Camardelli, and R. Malvezzi, "Digital twin for urban planning in the green deal era: A state of the art and future perspectives," *Sustainability*, vol. 14, no. 10, p. 6263, May 2022.

[25] Y. Ham and J. Kim, "Participatory sensing and digital twin city: Updating virtual city models for enhanced risk-informed decision-making," *J. Manag. Eng.*, vol. 36, no. 3, May 2020, Art. no. 04020005.

[26] Z. Allam, A. Sharifi, S. E. Bibri, D. S. Jones, and J. Krogstie, "The metaverse as a virtual form of smart cities: Opportunities and challenges for environmental, economic, and social sustainability in urban futures," *Smart Cities*, vol. 5, no. 3, pp. 771–801, Jul. 2022.

[27] Z. Shen et al., "Progress of flexible strain sensors for physiological signal monitoring," *Biosensors Bioelectron.*, vol. 211, Sep. 2022, Art. no. 114298.

[28] Y. Li, Y. A. Samad, T. Taha, G. Cai, S.-Y. Fu, and K. Liao, "Highly flexible strain sensor from tissue paper for wearable electronics," *ACS Sustain. Chem. Eng.*, vol. 4, no. 8, pp. 4288–4295, Aug. 2016.

[29] H. W. Choi et al., "Smart textile lighting/display system with multifunctional fibre devices for large scale smart home and IoT applications," *Nature Commun.*, vol. 13, no. 1, p. 814, Feb. 2022.

[30] J.-H. Pu et al., "Multilayer structured AgNW/WPU-MXene fiber strain sensors with ultrahigh sensitivity and a wide operating range for wearable monitoring and healthcare," *J. Mater. Chem. A*, vol. 7, no. 26, pp. 15913–15923, 2019.

[31] J. Eom et al., "Highly sensitive textile strain sensors and wireless user-interface devices using all-polymeric conducting fibers," *ACS Appl. Mater. Interfaces*, vol. 9, no. 11, pp. 10190–10197, Mar. 2017.

[32] L.-T. Hsu et al., "UrbanNav: An open-sourced multisensory dataset for benchmarking positioning algorithms designed for urban areas," in *Proc. 34th Int. Tech. Meeting Satell. Division Inst. Navigat.*, Oct. 2021, pp. 226–256.

[33] A. Leal-Junior, L. Avellar, V. Biazi, M. S. Soares, A. Frizera, and C. Marques, "Multifunctional flexible optical waveguide sensor: On the bioinspiration for ultrasensitive sensors development," *Opto-Electron. Adv.*, vol. 5, no. 10, 2022, Art. no. 210098.

[34] S. Gong et al., "A wearable and highly sensitive pressure sensor with ultrathin gold nanowires," *Nature Commun.*, vol. 5, no. 1, pp. 1–8, Feb. 2014.

[35] T. Q. Trung and N. Lee, "Flexible and stretchable physical sensor integrated platforms for wearable human-activity monitoringand personal healthcare," *Adv. Mater.*, vol. 28, no. 22, pp. 4338–4372, Jun. 2016.

[36] X. Wang, Z. Liu, and T. Zhang, "Flexible sensing electronics for wearable/attachable health monitoring," *Small*, vol. 13, no. 25, Jul. 2017, Art. no. 1602790.

[37] Y. Lei et al., "A MXene-based wearable biosensor system for high-performance in vitro perspiration analysis," *Small*, vol. 15, no. 19, May 2019, Art. no. 1901190.

[38] Y. Wu et al., "High resolution flexible strain sensors for biological signal measurements," in *Proc. 19th Int. Conf. Solid-State Sensors, Actuat. Microsystems*, Jun. 2017, pp. 1144–1147.

[39] A. Armgarth et al., "A digital nervous system aiming toward personalized IoT healthcare," *Sci. Rep.*, vol. 11, no. 1, p. 7757, Apr. 2021.

[40] Y. Hao, J. Wang, D. Huo, N. Guizani, L. Hu, and M. Chen, "Digital twin-assisted URLLC-enabled task offloading in mobile edge network via robust combinatorial optimization," *IEEE J. Sel. Areas Commun.*, vol. 41, no. 10, pp. 3022–3033, Oct. 2023.

[41] O. Chukhno, N. Chukhno, G. Araniti, C. Campolo, A. Iera, and A. Molinaro, "Placement of social digital twins at the edge for beyond 5G IoT networks," *IEEE Internet Things J.*, vol. 9, no. 23, pp. 23927–23940, Dec. 2022.

[42] Z. Zhang et al., "Deep learning-enabled triboelectric smart socks for IoT-based gait analysis and VR applications," *Npj Flexible Electron.*, vol. 4, no. 1, p. 29, Oct. 2020.

[43] W. Y. B. Lim et al., "Realizing the metaverse with edge intelligence: A match made in heaven," *IEEE Wireless Commun.*, vol. 30, no. 4, pp. 64–71, 2023.

[44] X. Shen, J. Gao, W. Wu, M. Li, C. Zhou, and W. Zhuang, "Holistic network virtualization and pervasive network intelligence for 6G," *IEEE Commun. Surveys Tuts.*, vol. 24, no. 1, pp. 1–30, 1st Quart., 2022.

[45] J. Wang, Y. Hao, L. Hu, T. Zhang, X. Ma, and M. Chen, "Self-maintained network digital twin for human-centric wireless metaverse," *IEEE Netw.*, early access, doi: 10.1109/MNET.2023.3337644.

[46] Q. Zhu, M. Y. Sarwar Uddin, N. Venkatasubramanian, and C.-H. Hsu, "Spatiotemporal scheduling for crowd augmented urban sensing," in *Proc. IEEE INFOCOM Conf. Comput. Commun.*, Apr. 2018, pp. 1997–2005.

[47] T. Haarnoja, A. Zhou, P. Abbeel, and S. Levine, "Soft actor-critic: Off-policy maximum entropy deep reinforcement learning with a stochastic actor," in *Proc. Int. Conf. Mach. Learn.*, 2018, pp. 1861–1870.

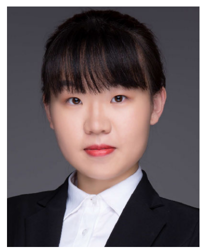

Jiaxi Wang received the bachelor's degree in automation from the College of Control Science and Engineering, Shandong University, Jinan, China, in 2021. She is currently pursuing the Ph.D. degree with the Embedded and Pervasive Computing (EPIC) Laboratory, School of Computer Science and Technology, Huazhong University of Science and Technology (HUST), Wuhan, China.

Her current research interests include edge computing and digital twin.

Yixue Hao (Member, IEEE) received the Ph.D. degree in computer science from the Huazhong University of Science and Technology (HUST), Wuhan, China, in 2017.

He is an Associate Professor at the School of Computer Science and Technology, HUST. His current research interests include 5G network, the Internet of Things, edge computing, edge caching, and cognitive computing.

Long Hu was a Visiting Student at the Department of Electrical and Computer Engineering, University of British Columbia, Vancouver, BC, Canada, from August 2015 to April 2017. He is an Associate Professor at the School of Computer Science and Technology, Huazhong University of Science and Technology (HUST), Wuhan, China. His research interests include the Internet of Things, software defined networking, caching, 5G, body area networks, body sensor networks, and mobile cloud computing.

Giancarlo Fortino (Fellow, IEEE) received the Ph.D. degree in systems and computer engineering from the University of Calabria (UNICAL), Arcavacata, Italy, in 2000.

He is currently a Full Professor of Computer Engineering with the Department of Informatics, Modeling, Electronics, and Systems, UNICAL. He is also a Guest Professor with the Wuhan University of Technology, Wuhan, China; a High-End Expert with the Huazhong University of Science and Technology, Wuhan; and a Senior Research Fellow with the Italian National Research Council ICAR Institute, Calabria, Italy. He is a (Founding) Series Editor of IEEE Press Book Series on *Human-Machine Systems* and the Springer series on *Internet of Things*. From 2002 to 2022, he was a Highly Cited Researcher by Clarivate in computer science. He has authored or coauthored more than 600 papers in international journals, conferences, and books. His research interests include wearable computing systems, IoT, and cyber-security.

Dr. Fortino is a member of the IEEE SMCS BoG and the Co-Chair of the SMCS TC on IWCD. He is the Chair of the IEEE SMCS Italian Chapter. He is an AE of premier IEEE TRANSACTIONS, such as IEEE TRANSACTIONS ON AUTOMATION SCIENCE AND ENGINEERING, IEEE TRANSACTIONS ON HUMAN-MACHINE SYSTEMS, IEEE INTERNET OF THINGS JOURNAL, IEEE SYSTEMS JOURNAL, IEEE TRANSACTIONS ON AFFECTIVE COMPUTING, *Information Fusion*, *Journal of Network and Computer Applications*, and *Engineering Applications of Artificial Intelligence*.

Salman A. Alqahtani is currently a Full Professor with the Department of Computer Engineering, College of Computer and Information Sciences, King Saud University, Riyadh, Saudi Arabia. He also serves as a senior consultant in computer communications, integrated solutions, and digital forensics for few development companies, and government sectors in Saudi Arabia. His main research interests include radio resource management (RRM) for wireless and cellular networks (4G, 5G), the Internet of Things (IoT), Industry 4.0, and digital forensics.

Min Chen (Fellow, IEEE) was an Assistant Professor with the School of Computer Science and Engineering, Seoul National University, Seoul, South Korea. He is a Full Professor with the School of Computer Science and Engineering, South China University of Technology, Guangzhou, China. He is also the Director of the Embedded and Pervasive Computing (EPIC) Laboratory, Huazhong University of Science and Technology (HUST), Wuhan, China. His Google scholar citations reached more than 43 400 with an H-index of 97. His top paper was cited more than 4500 times.

Dr. Chen is a Fellow of IET. He received the IEEE Communications Society Fred W. Ellersick Prize in 2017, the IEEE Jack Neubauer Memorial Award in 2019, and the IEEE ComSoc APB Oustanding Paper Award in 2022. He was selected as a Highly Cited Researcher from 2018 to 2023. He is the Founding Chair of the IEEE Computer Society Special Technical Communities on Big Data. He is the Chair of the IEEE Globecom 2022 eHealth Symposium.